



# Diode laser based gas analyzer for the simultaneous measurement of CO<sub>2</sub> and HF in volcanic plumes

Antonio Chiarugi<sup>1,2</sup>, Silvia Viciani<sup>2</sup>, Francesco D'Amato<sup>2</sup>, and Mike Burton<sup>3</sup>

<sup>1</sup>INGV, Pisa, Italy

<sup>2</sup>CNR - National Institute of Optics, Firenze, Italy

<sup>3</sup>University of Manchester, School of Earth and Environmental Science, Manchester, UK

*Correspondence to:* Francesco D'Amato ([francesco.damato@ino.it](mailto:francesco.damato@ino.it))

**Abstract.** A portable analyzer, for simultaneous detection of CO<sub>2</sub> and HF emitted by volcanoes and fumaroles, is described. The system is based on two fiber coupled Distributed FeedBack lasers and only one multipass cell, and provides the absolute concentration values of the 2 gases, without requiring a calibration procedure, at a maximum rate of 4 Hz. The spectrometer can operate both in a closed-cell configuration and in an open-cell setup, to remove all the problems connected with the chemisorption of the HF molecule. The concept, the practical realization and the laboratory performances of the device will be described. Moreover the results obtained during a first test campaign at the crater of Vulcano volcano will be reported, to demonstrate the in-field performances of the spectrometer.

## 1 Introduction

The dynamics of magma storage and ascent are reflected in the composition and flux of gases released by active volcanoes. The major volatile species, H<sub>2</sub>O, CO<sub>2</sub>, SO<sub>2</sub>, HCl, HF all have pressure-dependent solubility profiles, producing significant variability in gas composition as a function of depth in the magmatic system, which is then further modulated by the degassing style. The viscosity of magma controls its flow dynamics, and this is in turn controlled by the dissolved water contents of the magma and vesicularity, producing complex non-linear relationships between magma ascent and degassing. The thermodynamics of phase changes from dissolved to exsolved volatiles and crystal formation, together with adiabatic expansion, all contribute to the evolution of magmatic temperature, providing a further feedback mechanism as viscosity is also highly dependent on temperature. Unravelling this complex behaviour is a fundamental aim of volcanological science, and a key underpinning for this research is precise and accurate measurement of gas compositions at the surface. A further important scientific outcome from such measurements is new insight into atmospheric chemistry processes occurring within volcanic plumes.

A variety of methods have been developed to measure volcanic gas compositions, all with individual strengths and weaknesses. Direct sampling by dissolving hot fumarolic gases into alkali solutions followed by laboratory analysis allows a complete chemical description of sampled gases, but cannot be easily performed in dilute volcanic plumes, and sampling may be hazardous. In-situ sensors such as MultiGas (Shinohara et al. , 2008) have allowed automated measurements of plume gas compositions, primarily CO<sub>2</sub> and S species, to be performed, but the range of gases which can be measured is currently limited, and very fast changes in gas composition are challenging to quantify due to slow and differing frequency response of commonly used



optical CO<sub>2</sub> and chemical-based S sensors. Drifting calibrations make traceability of long term installations challenging. Remote sensing using infrared or ultraviolet spectroscopy (Butz et al. , 2017) is effective for safe determination of plume gases, and has a key capacity to measure gas compositions during explosive activity, but requires large path amounts of gas, and is poorly suited for in-situ measurements. Tunable diode laser-based in-situ spectrometers may overcome the challenges of  
5 chemical sensors, allowing traceable, accurate and precise measurements, and many volcanic gases have accessible near- and mid-infrared absorption spectra. They can also work at high frequency (> 1 Hz), which is a requirement for airborne surveys where rapid changes in gas concentration are common. However, TDL instruments are usually bulky, delicate and ill-suited to the rigours of volcanological fieldwork. A final essential requirement for volcanic gas sensing is that multiple gases are measured in the same volume of gas at the same time, whilst avoiding chemisorption processes. This allows the direct determination of  
10 volcanic gas molar ratios, which are the key to unravelling volcanic processes.

In the context of the European Research Council project CO2Volc, which has the aim of improving our understanding of global emissions of CO<sub>2</sub> from volcanoes, we identified the need for a custom-built TDL platform for volcanological applications. This platform would allow multiple gases to be measured simultaneously at high frequency (at least 2-3 Hz) to permit airborne measurements, would have high precision and accuracy to allow dilute plumes to be measured, and would be compact, low-power  
15 and robust to allow easy field deployment with a variety of transport solutions, including backpacks, airplanes and drones. Here, we report on the first measurements of CO<sub>2</sub> and HF we conducted with the new CO2Volc TDL platform, which was tested in the laboratory and on fumaroles on Vulcano island, Italy. A key requirement for volcanological applications is the simultaneous measurement of multiple gas species, as it is the ratio of volcanic species which provides constraints on magma dynamics. The species CO<sub>2</sub> and HF are ideally suited for revealing magma dynamics, being two end-members for solubility in  
20 magmas; CO<sub>2</sub> is high insoluble, and becomes saturated at depths typically > 10 km, while the bulk of HF degassing occurs at very low pressures.

## 2 State of the art for in-situ volcanic gas measurement

The requirements for a successful and effective volcanic gas analyser are stringent. The instrument must be compact and light for field portability, but also robust enough to allow operation in hostile and harsh environments, such as high humidity,  
25 fluctuating temperature and high concentrations of acid gases. Moreover, volcanic gas sensors would ideally have low power requirements to allow prolonged field measurements and the capability to work unattended through remote control or fully autonomously. Finally these constraints must not limit instrumental performance, maintaining high selectivity (in order to identify specific volcanic gas species), high sensitivity (in order to quantify small changes in gas concentration) and response times of the order of 1 s (in order to detect true changes in gas composition when concentrations are fluctuating rapidly). In addition to  
30 all of these requirements, the detection of acid gases, such as HF, require further precautions due to the rapid chemisorption of acid molecules on surfaces of the instrument, precluding pumps and filters.

Several laser spectrometers have been developed to measure multi-species gas emissions (Richter et al. , 2000, 2002) but these were poorly suited for the challenging volcanological field context, in particular for the key requirement of simultaneous mea-



5 measurement of multiple gas species and for the problems connected with chemisorption. Several analyzers fulfill the requirements for CO<sub>2</sub> and H<sub>2</sub>O measurements (Gianfrani et al. , 2000; Rocco et al. , 2004). In the market there is at least one commercial device for the simultaneous detection of both gases (LI-COR Li-7000). This device yields an accuracy of 1% for both gases, with a RMS noise of 25 ppb for CO<sub>2</sub> and 2 ppm for H<sub>2</sub>O at 1 s integration time. Its weight is less than 9 kg, and the power consumption is within 40 W. However, this device requires that gases are pumped through a narrow tube, which makes simultaneous measurement together with acid gases impossible.

10 Hydrogen fluoride could be measured using Cavity Ring-down Spectroscopy (CRDS) (Morville et al. , 2004), but low pressure operation is needed which is extremely challenging to achieve without experiencing strong chemisorption. Several other commercial devices offer HF detection, but none of them fulfills all the requirements for volcanological applications. The simplest ones are those used in human exposure monitoring (GfG), but the response time is too long (~90 s) and the cross sensitivity, in particular to hydrogen chloride (which is typically also present in volcanic plumes) is very strong. In Fourier Transform Infrared (FTIR) spectrometers, as in (Environnement), the detection limit is rather high (about 180 ppb with a time response of 2 s), and typically a multipass cell is needed for in-situ measurement which can provide a chemisorption surface. A higher sensitivity (2 ppb) can be reached with Ion Mobility Spectrometry (IMS) (Molecular Analytics), but again weight (23 kg) and power consumption (more than 500 W) are too high. Very high sensitivity can be obtained with Off-Axis Integrated Cavity Output Spectroscopy (ABB-Los Gatos) (detection limit of 0.2 ppb in 1 s, but with a power consumption of about 100 W and a weight of about 29 kg). Overall, we determined that none of these commercially available solutions were suitable for volcanological applications, as their weight, power and chemisorption characteristics don't fit our constraints. Furthermore, our specific requirements include measuring combinations of several volcanic gas species, such as CO<sub>2</sub> and HF, in the same volume of air, and devices like these do not exist on the market.

25 In view of the design requirements for volcanological applications, we have designed, produced and tested a new portable diode laser spectrometer for the simultaneous in-situ measurement of CO<sub>2</sub> and HF. As we show here, the new instrument has been designed to balance the competing requirements of low weight and power consumption, physical robustness and the required selectivity, sensitivity and time response performance. We have adopted direct absorption in combination with a multi-pass cell as a detection technique which, though noisier and less sensitive with respect to CRD or ICOS, allows a great simplification of the apparatus and doesn't need extremely high reflectivity of the cell mirrors. The latter was a source of concern as we will have the option of using the optical cells in open air.

30 The optical setup, based on two fiber coupled distributed feedback lasers (DFB) but only one home-made multipass cell, has been thought to optimize the instrument size and to reduce the weight to only 8-9 Kg. Moreover, such a setup insures that both laser beams run the same path and probe the same air in the same experimental conditions, so making this apparatus particularly suitable for simultaneous measurement of two gases concentration and for the estimation of their ratio.

35 The analyzer can work completely unattended and, if necessary, remotely controlled via Wi-Fi, for several hours in battery mode, with a power consumption lower than 50 W. The simultaneous absolute concentration values of the 2 gases, without calibration procedure, can be provided at a maximum rate of 4 Hz. We have addressed the problem of chemisorption of HF



with two possible configurations of the spectrometer: a closed-cell configuration, with a teflon tube enclosing the multipass cell and a pump system to inject air into the cell, and an open-cell configuration to reduce the contact between the gas and the surfaces of the instrument. The practical realization and the laboratory performances of the device, with an Allan-Werle Variance analysis will be described. Finally, the results obtained during a first test campaign at the crater of Vulcano volcano (Aeolian Islands, Italy) will show an in-field detection limit of 320 ppb for CO<sub>2</sub> and of 20 ppb for HF with an integration time of 2 s.

### 3 Experimental setup

The optical setup of the analyzer is based on two near-IR DFB fiber coupled diode lasers and only one multipass cell (Fig. 1). In order to optimize the instrument size and to better exploit the available space, the laser sources and the entrance of the cell are on one side (“top”) of the optical breadboard, while the reference arm, the detectors and the exit of the cell are on the other side (“bottom”).

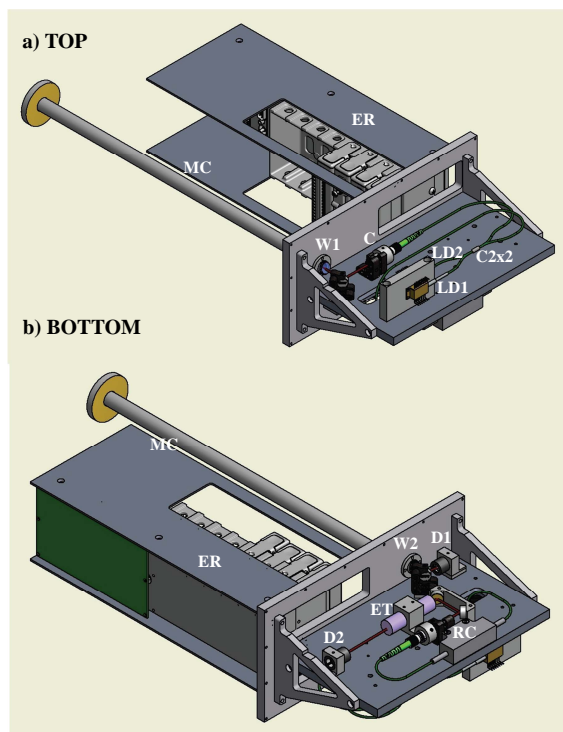


**Figure 1.** Optical scheme of the analyzer. a) Top view. LD1 and LD2 diode lasers; C2x2: fiber coupler 2x2 50/50 transmission; C: collimator; W1: CaF<sub>2</sub> window for the entrance of the multipass cell MC. b) Bottom view. RC: reference cell; ET: BK7 etalon; W2: CaF<sub>2</sub> window for the output of the multipass cell MC; D1 and D2 detectors. ER: rack for electronics



On the top side of the breadboard, two fiber coupled DFB lasers emitting respectively at  $1.278\ \mu\text{m}$  and  $2.004\ \mu\text{m}$  (Eblana Photonics EP1392-DM and EP2000-DM, output power 5 mW and 2 mW) are directly mixed in a “2x2” fiber coupler, 50/50 transmission, working around  $1.3\ \mu\text{m}$  and  $1.5\ \mu\text{m}$  (Thorlabs 10202A-50-APC). As a matter of fact, this component is a standard one and in principle is not dichroic for the two laser wavelengths. Nevertheless we don’t need an exact splitting ratio, and the attenuation of the coupler at  $2\ \mu\text{m}$  is low enough to allow us to exploit it. So about half of the power of both lasers is collimated and sent into the multi-pass cell, while the other half of the power of the two beams is sent towards the bottom side of the breadboard.

The multipass cell (Fig. 2) is a home made cell with a total pathlength of 20.23 m in 52 passes. It has two quartz mirrors mounted on a carbon fiber pipe. The pipe is kept by a stainless steel holder, which can be fixed to the analyzer body in a repeatable way by means of three spines. This allows a fast and easy mounting and removal of the cell in case of cleaning or replacement. As several identical cells have been aligned in the same optical setup, in case of replacement no realignment of the analyzer is necessary, and just the orientation of the final mirror could require to be optimized. The beam enters the multipass cell and gets back into the analyzer across two  $\text{CaF}_2$  windows, tilted by an angle of  $19^\circ$  in order to avoid interference fringes.

On the bottom side of the breadboard, the beams exiting from the multipass cell is sent to a 20 mm plano convex lens and focused onto a main detector (Hamamatsu G12183-010K, InGaAs PIN,  $0.9\text{--}2.6\ \mu\text{m}$ ,  $\phi\ 1\ \text{mm}$ , uncooled), which is suitable for both laser wavelengths.

The other beams exiting from the 2x2 coupler are sent across a reference cell (manufactured by Wavelength References), containing both HF and  $\text{CO}_2$ , to verify the right settings of the two lasers, in particular for HF, which is usually absent in the atmosphere. The reference beam is then collimated and sent through a custom-built etalon in order to obtain a relative frequency reference for the linearization and calibration of the frequency scale. The etalon is made from BK7, 6 cm long and with Free Spectral Range (FSR)  $0.0554/0.0558\ \text{cm}^{-1}$  at 1278 and 2004 nm, respectively. Finally, the reference signal is measured with a detector identical to that used in the measurement channel.

All the electronics is placed aside the cell (as shown in Fig. 1). The core of the instrument is a CompactRIO crate by National Instruments (cRIO 9074), which combines a dual-core processor, a reconfigurable FPGA, and five commercial plug-ins for fast acquisition (four independent channels, 1 MHz at 16 bits), slow acquisition (8 multiplexed channels, 500 kHz at 12 bits), digital I/O, thermocouple reading and data storage. Laser current drivers, laser temperature controllers and preamplifiers for detectors are home made.

In order to protect optics and electronics against the volcanic gases, they are enclosed within a plastic cover, sealed with a rubber O-ring on the aluminum breadboard of the instrument. This means that HF is measured only in the volume of the multipass cell, but  $\text{CO}_2$  is inside the plastic cover too. However, due to the choice of optics fibers components, inside the box the main beam travels in the air only from the collimator to the first  $\text{CaF}_2$  window, and from the second window to the main detector. This pathlength is in total 11.5 cm, to be compared to about 20 m. So by neglecting this path, we would overestimate



the ambient concentration of CO<sub>2</sub> of only about 6·10<sup>-3</sup>.

The device can operate in an open-cell configuration (as in Fig. 2a) or in a closed-cell configuration (as in Fig. 2b). In the first case, we don't need any sampling air mechanism and the acquisition time is not limited by the time necessary to completely refresh the air inside the cell volume. In the latter, the cell is closed with a teflon tube and the air is sampled by a rotary pump, which provides an average flow of 20 l/min. So the 1-l volume of the multipass cell is flushed in about ~ 3 s.



**Figure 2.** Home made multipass cell in the open-cell configuration (a) and in the closed-cell configuration (b).

The pressure and the temperature inside and outside the cell are measured respectively by a silicon piezoresistive pressure sensor (Motorola, MPX2100A, with accuracy of about 1%) and by a PT100 sensor (National Instruments, NI 9217 RTD, with accuracy of about 0.8%).

The total power requirement for the normal operation of the spectrometer is about 20-25 W (in the open-cell configuration without pump) and 50 W (in the closed-cell configuration with pump). The power is provided by one (open-cell configuration) or two (closed-cell configuration) 4-cells LiPo batteries, 6800 mAh at 14.8 V.

The instrument is robust and compact (with size of 60.5x27.6x13.2 cm), with a weight of about 8-9 Kg (pump and batteries included), that makes it particularly suitable as a portable instrument for in-situ operation in a hostile ambient as the volcanic area. The spectrometer can work for about 4-5 hours completely unattended and, if the case, remotely controlled via Wi-Fi, far from the dangerous area of the toxic gases emission.

#### 4 Acquisition technique and data processing

The concentration values of the two gases are inferred by the absorption signals registered by the main detector, according to the Beer-Lambert law. The absorption signals are obtained by scanning the two lasers emission frequencies across the absorptions of the target molecules, by modulating the laser current with a ramp signal. The 1.3 μm-laser is scanned over the HF absorption





at  $7823.82 \text{ cm}^{-1}$ , while the  $2 \mu\text{m}$ -laser scans over the  $\text{CO}_2$  absorption at  $4989.97 \text{ cm}^{-1}$ .

The two laser sources work in sequence and are switched on alternatively: when one laser is switched off, the current of the other laser is modulated, and conversely. The time interval between the two laser scans is 2 ms, so that the two measurements can be considered simultaneous for the purposes of our applications. The modulation signal of each laser consists of 3 parts:

5 a linear ramp with a duration of 1.6 ms; a region of  $100 \mu\text{s}$  during which the laser is turned off to get the detector zero-power signal; and a region of  $300 \mu\text{s}$  during which the laser current is maintained fixed at the starting value of the ramp, to allow the stabilization of the signal before starting the frequency scan. The repetition frequency for the complete sequence of ramps is about 250 Hz. The maximum tuning of the two lasers provides two frequency scans of  $0.8 \text{ cm}^{-1}$  around  $\text{CO}_2$  and  $1.5 \text{ cm}^{-1}$  around HF, respectively.

10 The zero-power signal allows to know the absorption independently from the absolute value of the laser power, consequently we don't need to know exactly the splitting ratio of the beam splitter and we can face changes of reflectivity of the mirrors, related to the interaction with the external ambient.

The reference and main signals are acquired synchronously on 2 channels at 1 MSample/s with a resolution of 16 bits. Each 4000-points main signal, which consists of the two absorption spectra and each 4000-points reference signal, are averaged 25  
15 times and saved for a post-processing. Also pressure and temperature are saved together with each acquisition. If the time for saving data is also considered, the acquisition time for the simultaneous absorption spectra of  $\text{CO}_2$  and HF is of 0.25 s.

A detailed description of the data processing can be found in (Viciani et al., 2008). The absorption spectra, after subtracting the zero-power signal, is fitted with the exponential of a Voigt profile multiplied by a two-order polynomial, which simulates the sloping background due to the ramping of the driving current. We use as Voigt profile the four-Lorentz Puerta–Martin  
20 approximation (Puerta et al. , 1981; Martin et al. , 1981), where the only free fitted parameters are the line amplitude and center frequency, while the Lorentzian and Gaussian half widths at half maximum (HWHM) are maintained fixed. The values of the HWHM are calculated as a function of temperature and pressure, measured for each acquisition, and of the molecular parameters according to the HITRAN database ((Rothman et al. , 2013)). Obviously, the frequency calibration of the x-axis becomes essential for this approach so that, for each saved absorption spectrum, the corresponding reference signal is recorded  
25 and fitted according to the etalon transmission equation, multiplied for a two-order polynomial and for the absorption signal of the reference cell. According to the fit results, and knowing the etalon FSR, the frequency scale can be determined for each acquisition.

The integrated absorbance for the two molecules is calculated according to the fitting parameters of the Voigt function, and the concentration  $N$  is calculated from the absorbance knowing the multipass path length and the gas line-strength of  $\text{CO}_2$  and  
30 HF, according to the HITRAN database (Rothman et al. , 2013). Finally, the mixing ratio  $MR$  is obtained according to the Equation:

$$MR = \frac{N}{N_0} \frac{T}{T_0} \frac{P_0}{P} \quad (1)$$



where  $N$  is the calculated molecules concentration in  $\text{cm}^{-3}$ ,  $P$  and  $T$  are the measured values of pressure (in atm) and temperature (in K),  $P_0=1$  atm,  $T_0=296$  K and  $N_0=2.470 \times 10^{19} \text{ cm}^{-3}$ .

## 5 Laboratory performances of the instrument for the CO<sub>2</sub> channel

5 In order to test the laboratory performances of the instrument and to verify the reliability of the inferred concentration values, a mixture of known concentration has been used in the closed-cell configuration. Such kind of test, if done with an HF mixture, would be deeply influenced by the property of the acid HF to stick, inside the tube closing the cell or inside the pipes connecting the multipass cell to the tank of the mixture. We have also verified (as shown in the next session) that, by using teflon sampling pipes, the problem is reduced but not completely resolved, due to chemisorption of HF to water vapor film or dust covering the  
10 inside of the tubes. Consequently, we have decided to carry out this laboratory test only for the CO<sub>2</sub> channel and to evaluate the performances of the HF part directly in-field by using the open-cell configuration.

A calibrated mixture of CO<sub>2</sub> at 591 ppm ( $\pm 3$  ppm) in synthetic air has been used.

The measurement has been carried out by introducing into the multipass cell a constant flow of mixture (about 0.3 l/min) at atmospheric pressure and also at 700 mBar, to simulate a typical pressure at the top of a 3000 m volcano (e.g. Etna). We show  
15 in Fig. 3 a normalized absorption spectrum of the CO<sub>2</sub> mixture, detected by our instrument at the maximum rate of 4 Hz, at atmospheric pressure and at a temperature of about 295 K. The results of the Voigt fitting procedure and the corresponding residuals are also shown in Fig. 3. Two optical fringes are also included in the fitting curve.

In order to determine the accuracy of the measurement we followed the same formalism described in (Viciani et al., 2008). The mixing ratio uncertainty is essentially determined by the following contributions: the accuracy of the temperature and  
20 pressure measurement (respectively 1% and 0.8%), the accuracy of the CO<sub>2</sub> line strength according to the HITRAN database (between 1% and 2%) (Rothman et al., 2013) and the uncertainty in the fitting procedure (0.2%). The resulting total accuracy is  $< 4\%$ .

From the spectra of Fig. 3 we retrieve a CO<sub>2</sub> mixing ratio of  $(592 \pm 12)$  ppm. This value is in agreement with the concentration of the calibrated mixture.

25 In order to evaluate the long-term stability of the instrument, we have repeated the same measurement, at a rate of 4 Hz, for about 1 hour, in both conditions of atmospheric pressure and about 700 mBar.

Assuming as precision the standard deviation ( $2\sigma$ ) of the obtained concentration values, we infer a CO<sub>2</sub> precision for 1-hour measurement of 0.1% (600 ppb) at atmospheric pressure and of 0.03% (200 ppb) at lower pressure. This higher precision can be explained because at lower pressure the absorption signals are narrower and it is easier for the fitting protocol to clearly  
30 identify the background signal and the optical fringes.

Moreover, in order to evaluate the ultimate sensitivity of the the CO<sub>2</sub> channel, an Allan-Werle Variance analysis of the obtained concentration values has been carried out. An Allan-Werle Variance plot of the CO<sub>2</sub> concentration measurements is reported in Fig. 4 as a function of the integration time.



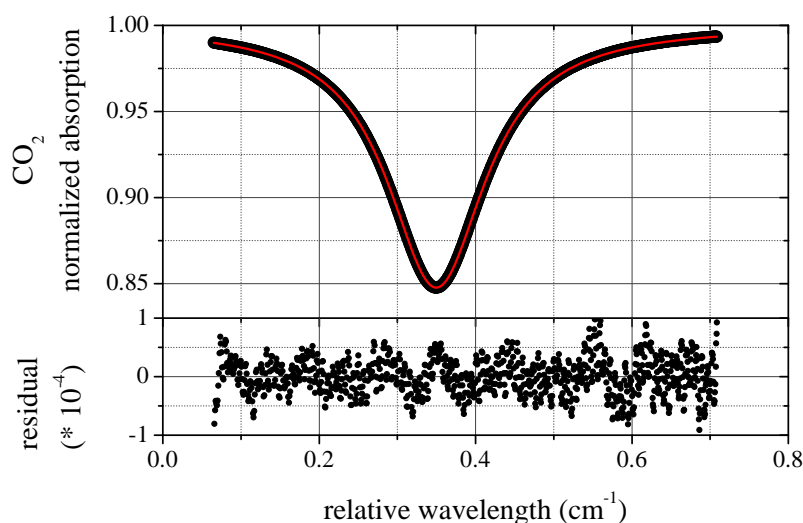


**Figure 3.** Normalized absorption spectra of a CO<sub>2</sub> calibrated mixture (of about 590 ppm in synthetic air) around 4989.97 cm<sup>-1</sup> and Voigt fit results (red line). The residuals of the fitting procedure are shown in the bottom part. The acquisition time is 0.25 s. The measurement has been carried out at ambient pressure and at a temperature of 295 K.

We can conclude that the CO<sub>2</sub> sensitivity at the fastest acquisition time of the instrument (250 ms) is about 500 ppb at atmospheric pressure and less than 100 ppb at lower pressure. For an integration time of 1 s, a detection limit of about 300 ppb at atmospheric pressure and of about 60 ppb around 700 mbar, is obtained. The best achievable sensitivity for the CO<sub>2</sub> channel can be reached for 110 s of integration time (about 80 ppb) at atmospheric pressure and for 30 s of integration time (about 15 ppb) at 700 mbar. Again, we believe that this reduction of the best integration time at low pressures is due to the better capability of the system to get rid of fringes.

## 6 In-field performances of the instrument for CO<sub>2</sub> and HF channels

Two test campaigns have been carried out in order to evaluate the performance of the instrument and in particular of HF measurement, as this is the most sensitive to chemisorption processes.

- 10 The first campaign was performed in April 2015 at the crater of Vulcano volcano (Aeolian Islands, Italy). During this campaign the instrument was deployed in the closed-cell configuration, with ambient pumped through a 1 m Teflon tube into the cell (as in Fig. 2b). The integration time for each measurement was 1.5 s. We placed the instrument downwind of degassing fumaroles, producing exposure to a variety of gas concentrations.

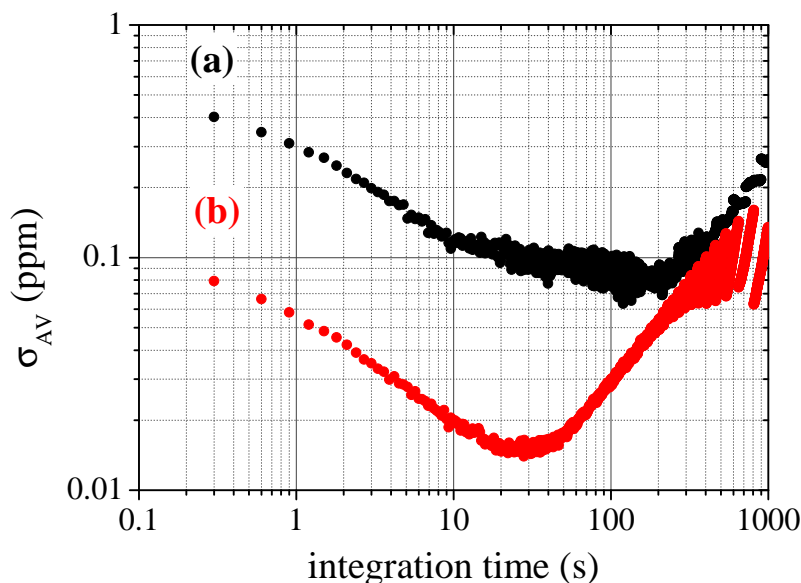


**Figure 4.** Allan-Werle Variance plot of 1 hour in-flow measurements of a CO<sub>2</sub> calibrated mixture of about 590 ppm in synthetic air, at a rate of 4 Hz in two different conditions: for a pressure of 985 mbar and a temperature of 295 K (curve a) and for a pressure of 687 mbar and a temperature 294 K (curve b).

The results obtained for about 10 minutes of concentration measurement of HF and CO<sub>2</sub> are reported in Fig. 5. A correlation between the concentration peaks of different gases is observed, but the peaks are not well aligned in general, and the HF peaks show a significant delay compared with CO<sub>2</sub>. Correlation analysis of the two concentrations clearly shows that a maximum correlation between the two gases is reached for a delay of about 16 s. Moreover, the correlation is poor with a maximum correlation coefficient of only 30%. We attribute these observations to chemisorption of HF molecules, which stick inside the pipes or inside the tube covering the cell, in spite of the use of teflon components. When an emission peak arrives to the pipe inlet, part of the HF is lost as it reacts with the walls, producing a delayed HF peak. The only way to solve completely this problem is to remove all the pipes and the tube covering the cell.

The open-cell configuration has been employed in a second campaign, also at the crater of Vulcano volcano, performed during May 2015.

A typical normalized absorption spectrum for both CO<sub>2</sub> and HF, with 2 s integration time for each measurement, is shown in Fig. 6. The measurement has been carried out close to a fumarole of the volcano, with a pressure of 990 mbar and a temperature changing between 310 K and 320 K. The results of the Voigt fitting procedure and the corresponding residuals are also shown in Fig. 6. Three optical fringes for CO<sub>2</sub> and two optical fringes for HF are also included in the fitting curve.

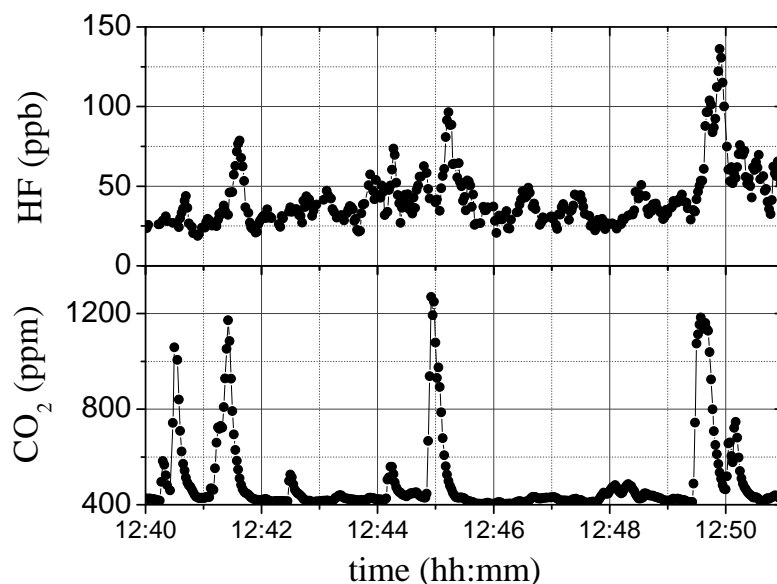


**Figure 5.** Time series of CO<sub>2</sub> and HF concentrations measured at the crater of Vulcano volcano on the 22nd April 2015, performed by the spectrometer in the closed-cell configuration. The measurements have been carried out in an average condition of 990 mbar of pressure and 300 K of temperature. The integration time is 1.5 s. The delay in the acquisition times of the HF peaks with respect to the CO<sub>2</sub> peaks is due to the closed-cell configuration.

The accuracy of the concentration values is determined by the same parameters described in the previous section: the uncertainties on temperature, pressure and CO<sub>2</sub> line strength are the same as in the laboratory test; the accuracy of the HF line strength according to the HITRAN database is between the 10% and 20% (Rothman et al. , 2013); the uncertainty of the fitting procedure is 0.2% for CO<sub>2</sub>, exactly the same as in the laboratory test reported in Fig. 3, and 0.7% for HF. The resulting total accuracy is <4% for CO<sub>2</sub> and <22.5% for HF. The low accuracy for HF is mainly due to the large uncertainty of the line strength reported in the HITRAN database. By assuming the worst uncertainty, the CO<sub>2</sub> concentration value for the spectrum of Fig. 6a is  $(2350 \pm 50)$  ppm and the HF concentration value for the spectrum of Fig. 6b is  $(4.5 \pm 0.5)$  ppm.

The advantage of the open-cell configuration, with respect to the closed-cell employed in the previous campaign, becomes obvious when a correlation analysis between the two gases is performed. The delay of the HF peaks with respect to the CO<sub>2</sub>, observed in Fig. 5, is now absent and a maximum correlation between the two gases is obtained without introducing any delay. The CO<sub>2</sub> concentration as a function of the HF concentration during 13 minutes of measurement is reported in Fig. 7 and the linearity indicates a high correlation between the two gases, corresponding to a correlation coefficient of 95%. This high correspondence is better shown in the inset of Fig. 7, where a zoom of the simultaneous time series of CO<sub>2</sub> and HF during a 3-minutes interval is displayed.

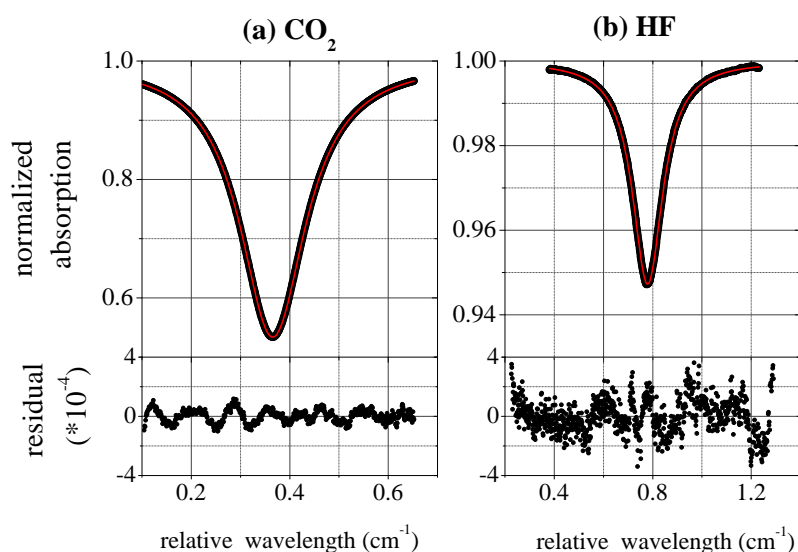


**Figure 6.** Typical normalized absorption spectra of CO<sub>2</sub> (a) and HF (b) detected in proximity of a fumarole of the Vulcano volcano on the 20th May 2015 and Voigt fit results (red line). The residuals of the fitting procedure are shown in the bottom parts. The concentration value of CO<sub>2</sub> is 2350 ppm and the concentration value of HF is 4.5 ppm. The acquisition time is 2 s. The measurement has been carried out at a pressure of 990 mbar and at a temperature of 312 K.

A linear fit of the data of Fig. 7 allows to infer both the CO<sub>2</sub> ambient concentration not due to volcanic emissions (calculated as the CO<sub>2</sub> value when the measured HF is zero), and the ratio between the CO<sub>2</sub> and HF concentrations. The obtained results are  $(390 \pm 20)$  ppm for the CO<sub>2</sub> ambient concentration and  $(460 \pm 50)$  for CO<sub>2</sub>/HF ratio.

In order to evaluate the in-field sensitivity of the instrument we assume as signal-to-noise ratio  $S/N$  the ratio between the normalized absorption signal and two times the standard deviation ( $2\sigma$ ) of the residual corresponding to the Voigt fit.

In Fig. 8 the  $S/N$  as a function of CO<sub>2</sub> and HF concentration is reported. We use as noise value for the data of Fig. 8 the mean value of the noise related to different fit results of the detected spectra, most of which show a residual similar to that one displayed in Fig. 6. The mean noise value is  $8.5 \cdot 10^{-5}$  for CO<sub>2</sub> and  $2.4 \cdot 10^{-4}$  for HF.

The sensitivity for the two channels of the spectrometer can be obtained as the concentration for which  $S/N = 1$ . It can be inferred from the linear fit of the data in Fig. 8. The obtained detection limit for the CO<sub>2</sub> channel, with an integration time of 2 s, is 320 ppb, which is only slightly higher with respect to the value of 250 ppb obtained during the Allan-Werle Variance laboratory test shown in Fig. 4. We can conclude that the sensitivity performances of the CO<sub>2</sub> analyzer are not seriously degraded by the in-field operation and they are reduced only by a factor of 1.3. Consequently, from the laboratory Allan-Werle Variance analysis we can estimate an in-field sensitivity, at the fastest integration time of 250 ms, of about 650 ppb and an in-field ultimate sensitivity (at 110 s of integration time) of about 100 ppb, which can be further increased if we work at lower

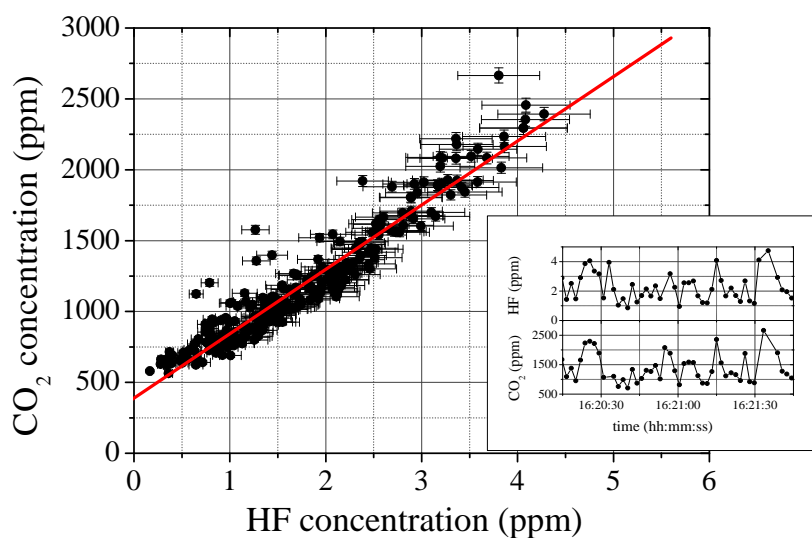


**Figure 7.** CO<sub>2</sub> concentration as a function of the HF concentration for 13 minutes of measurement in proximity of a fumarole of the Vulcano volcano on the 22nd April 2015. The red line is the result of a linear fit. The error bars are the accuracy of the concentration values. The measurement has been carried out in the open-cell configuration at a pressure of 990 mbar and at a temperature variable between 310 K and 320 K. The inset shows a zoom of the time series of CO<sub>2</sub> and HF during a 3-minutes interval.

pressure (about 20 ppb for an integration time of 30 s at a pressure of 700 mbar).

For the HF channel, a detection limit of 20 ppb, with an integration time of 2 s, can be obtained from the linear fit of Fig. 8b.

This performance can degrade over time as the mirrors of the multipass cell become dirty due to water, dust and gas emissions from the volcanic plumes, and the detected power is consequently drastically reduced. When the instrument operates very close to the fumaroles, in about 30 minutes the sensitivity of the spectrometer (for an integration time of 2 s) degrades to 2 ppm for CO<sub>2</sub> and to 200 ppb for HF. On the contrary, when the instrument is far from the fumaroles, or on board an aircraft, it can work indefinitely without significant reduction in performance.

In-situ degradation of the mirrors could be partially solved by keeping the mirrors clean with an air blade, where a light flux of air is blown through the carbon fiber pipe holding the mirrors. The air can be taken a few meters apart, far from the high concentrations at the emission points, and blown on the mirrors by using a pump with a dust filter at its inlet. Consequently, a small volume of air close to the mirrors will be filled with this purge air, where HF concentration is negligible and CO<sub>2</sub> concentration is close to its ambient level. This means that the effective distance between the mirrors is reduced. This reduction (estimated as lower than 3%) must be taken into account when concentration values are calculated. Moreover, for CO<sub>2</sub>, the values of concentration before or after each emission peak must be used to correct the peak values.

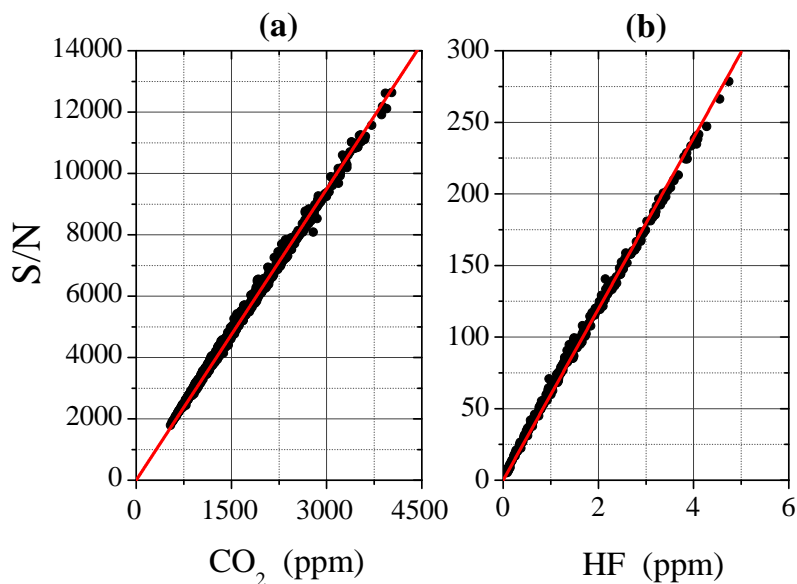


**Figure 8.** Signal-to-noise ratio  $S/N$  as a function of  $\text{CO}_2$  concentration (a) and HF concentration (b) for 13 minutes of measurement in proximity of a fumarole of the Vulcano volcano on the 22nd April 2015. The red line is the result of a linear fit. The measurement has been carried out in the open-cell configuration at a pressure of 990 mbar and at a temperature variable between 310 K and 320 K.

We have produced a new analyzer for the simultaneous measurement of the concentrations of  $\text{CO}_2$  and HF in volcanic gas emissions. This device features low weight and power, as well as resistance to the harsh environmental conditions. The in-field spectrometer sensitivity, obtained during a campaign at the crater of Vulcano, is 320 ppb for  $\text{CO}_2$  and 20 ppb for HF, for an integration time of 2 s. According to laboratory tests, this sensitivity decreases by about a factor 2 when the instrument is employed at its maximum rate of 4 Hz. However, the device performances improve when the measurements are carried out at a pressure lower than the atmospheric one. In particular the  $\text{CO}_2$  sensitivity increases of about a factor 5 when the pressure is reduced to 700 mbar, a typical pressure at the top of a 3000 m volcano (e.g. Etna). We are planning to extend the measurement to  $\text{H}_2\text{O}$ , by detecting a water absorption close to a  $\text{CO}_2$  one. This requires a higher tunability DFB laser at  $2 \mu\text{m}$ , which is under procurement.

10 *Acknowledgements.* The activity has been supported by the FP7-IDEAS-ERC Project CO2Volc (Grant 279802). The authors thank Mr. Marco De Pas, Mr. Mauro Giuntini and Mr. Alessio Montori for the realization of the non-commercial electronics, and Mr. Roberto Calzolari and Mr. Massimo D’Uva for the realization of mechanics. We greatly appreciate the support of Manuel Queisser, Giuseppe Salerno and Alessandro la Spina in performing the field measurements.





## References

- ABB - Los Gatos Research, Hydrogen Fluoride Analyzer, URL=[www.lgrinc.com](http://www.lgrinc.com)
- Butz, A., Dinger, A. S., Bobrowski, N., Kostinek, J., Fieber, L., Fischerkeller, C., Giuffrida, G. B., Hase, F., Klappenbach, F., Kuhn, J., Lübecke, P., Tirpitz, L., and Tu, Q.: Remote sensing of volcanic CO<sub>2</sub>, HF, HCl, SO<sub>2</sub>, and BrO in the downwind plume of Mt. Etna, Atmos. Meas. Tech., 10, 1-14, DOI=10.5194/amt-10-1-2017, 2017.
- 5 Environnement S.A., Model MIR FT, URL=<http://www.environnement-sa.com/products-page/en/emission-monitoring-en/multigas-stationary-monitoring-systems-en/mir-ft-2/?cat=120>.
- GfG Instrumentation, Model TN 2014 Micro IV, URL=<http://goodforgas.com/shop/micro-iv-single-gas-detector>.
- Gianfrani, L. De Natale, P., De Natale, G., Remote sensing of volcanic gases with a dfb-laser-based fiber spectrometer, Appl. Phys. B 70, 10 467-470, 2000.
- LI-COR, Model LI-7000, URL=[https://www.licor.com/env/products/gas\\_analysis/LI-7000](https://www.licor.com/env/products/gas_analysis/LI-7000)
- Martin, P., and Puerta, J., Generalized lorentzian approximations for the Voigt line shape, Appl. Opt., 20, 259-263, 1981.
- Molecular Analytics, Particle Measuring Systems, Model ProSentry-IMS HF Analyzer, URL=[www.pmeasuring.com](http://www.pmeasuring.com)
- Morville, J., Romanini, D., Kachanov, A. A., Chenevier, M., Two schemes for trace detection using cavity ringdown spectroscopy, Appl. 15 Phys. B 78, 465-476, DOI=10.1007/s00340-003-1363-8, 2004.
- Puerta, J. and Martin, P., Three and four generalized lorentzian approximations for the Voigt line shape, Appl. Opt., 20, 3923-3928, 1981.
- Richter D., Lancaster D. G., Tittel F. K.: Development of an automated diode laser based multicomponent gas sensor, Appl. Opt., 39, 4444-4450, 2000.
- Richter D., Erdelyi M., Curl R. F., Tittel F. K., Oppenheimer C., Duffell H. J., Burton M.: Field measurements of volcanic gases using tunable 20 diode laser based mid-infrared and fourier transform infrared spectrometers, Opt. Laser Eng. 37, 171-186, 2002.
- Rocco, A., De Natale, G., De Natale, P., Gagliardi, G., Gianfrani, L., A diode-laser-based spectrometer for in-situ measurements of volcanic gases, Appl. Phys. B, 78, 235-240, 2004.
- Rothman, L. S., Gordon, I. E., Babikov, Y., Barbe, A., Benner, D. C., Bernath, P. F., Birk, M., Bizzocchi, L., Boudon, V., Brown, L. R., Campargue, A., Chance, K., Cohen, E. A., Coudert, L. H., Devi, V. M., Drouin, B. J., Fayt, A., Flaud, J. M., Gamache, R. R., Harrison, 25 J. J., Hartmann, J. M., Hill, C., Hodges, J. T., Jacquemart, D., Jolly, A., Lamouroux, J., Roy, R. J. L., Li, G., Long, D. A., Lyulin, O. M., Mackie, C. J., Massie, S. T., Mikhailenko, S., Müller, H. S. P., Naumenko, O. V., Nikitin, A. V., Orphal, J., Perevalov, V., Perrin, A., Polovtseva, E. R., Richard, C., Smith, M. A. H., Starikova, E., Sung, K., Tashkun, S., Tennyson, J., Toon, G. C., Tyuterev, V. G., Wagner, G., The HITRAN 2012 molecular spectroscopic database, J. Quant. Spectrosc. Radiat. Transf., 130, 4-50, 2013.
- Shinohara, H., Aiuppa, A., Giudice, G., Gurrieri, S. and Liuzzo, M., Variation of H<sub>2</sub>O/CO<sub>2</sub> and CO<sub>2</sub>/SO<sub>2</sub> ratios of volcanic gases discharged 30 by continuous degassing of Mount Etna volcano, Italy, J. Geophys. Res., 113, B09203, DOI=10.1029/2007JB005185, 2008.
- Viciani, S., D'Amato, F., Mazzinghi, P., Castagnoli, F., Toci, G., Werle, P. W., A cryogenic operated diode-laser spectrometer for airborne measurement of stratospheric trace gases, Appl. Phys. B, 90, 581-592, 2008.